Wolf-Rayet Stars at the Highest Angular Resolution

Florentin Millour[1]
Olivier Chesneau[2]
Thomas Driebe[1]
Alexis Matter[2]
Werner Schmutz[3]
Bruno Lopez[2]
Romain G. Petrov[2]
José H. Groh[1]
Daniel Bonneau[2]
Luc Dessart[4]
Karl-Heinz Hofmann[1]
Gerd Weigelt[1]

[1] Max-Planck-Institut für Radioastronomie, Bonn, Germany
[2] Observatoire de la Côte d'Azur, Nice, France
[3] Physikalisches-Meteorologisches Observatorium Davos, World Radiation Center, Switzerland
[4] Observatoire de Paris, France

Interferometric observations of high-mass evolved stars provide new and very valuable information of their nature. With the unique capabilities of the VLTI, direct images of their closest environment where mass loss and dust formation occur, can be obtained. The breakthrough of the VLTI in terms of angular resolution as well as spectral resolution allows competing theoretical models, based on indirect constraints, to be tested. The high angular resolution made available by the VLTI shows that there is still a lot to discover about these massive stars.

Massive stars strongly influence their sur - roundings due to their extreme temperature, luminosity, and mass-loss rate. In addition, they are short-lived, and their fate is to explode as core-collapse supernovae. Among the extensive zoology of massive stars, Wolf-Rayet stars probably represent the last stage of stellar evolution, just before the explosion as a supernova. So far, Wolf-Rayet stars have been mainly studied by means of spectroscopy and spectropolarimetry, based on spatially unresolved observations. Nonetheless, there is extensive evidence of binarity and geometrical complexity of the nearby wind in many Wolf-Rayet stars. In this context, high angular resolution techniques fill the gap, since they can provide spatially resolved observations of massive stars and their immediate vicinity. However, the number of Wolf-Rayet stars in the solar vicinity is very low (Van der Hucht, 2001; Crowther, 2007). Therefore, all Wolf-Rayet stars are too remote to be spatially resolved by adaptive optics. However, for a handful of objects, the geometry of the innermost circumstellar structures (discs, jets, latitude-dependent winds, or even more complex features) can be directly probed with the highest spatial resolution available, through the use of stellar interferometry.

A closer look at Wolf-Rayet stars

Wolf-Rayet (WR) stars begin their life as massive objects (usually O-type supergiant stars) with at least 20 times the mass of the Sun. Their life is brief, and they die hard, exploding as supernovae and blasting vast amounts of heavy elements into space, which are recycled in later generations of stars and planets. By the time these massive stars are near the end of their short life, during the characteristic "Wolf-Rayet" phase, they develop a fierce stellar wind — a stream of particles ejected from the stellar surface by the radiative pressure — expelling mass at a tremendous rate (up to $10^{-3} M_{\odot}$/yr) while they are synthesising elements heavier than hydrogen in their cores. One of the characteristics of WR stars is the low hydrogen content of the atmosphere due to the stripping-off of the outer layers as a result of the strong mass loss. Before and during the WR phase, such stars eject a large amount of matter, more than $10 M_{\odot}$, and with velocities up to 3000 km/s, which then surrounds the central star in the form of gas and dust.

Theoretically, the evolution of a WR star ends with the collapse of its core and, as a rule, the formation of a black hole or a neutron star occurs. Energetic Type Ib and Ic supernovae (SNe) are thought to be direct descendants of massive WR stars (see, for instance, Crowther, 2007). It is now recognised that long-duration gamma-ray bursts (GRBs) are linked to the collapse of massive stars. The merging of the components in a binary system, including a rapidly rotating WR, is considered to be one of the channels leading to these extraordinary events, although this is not yet firmly established. Only ~ 1% of core-collapse SNe are able to produce a highly relativistic collimated outflow and, hence, a GRB.
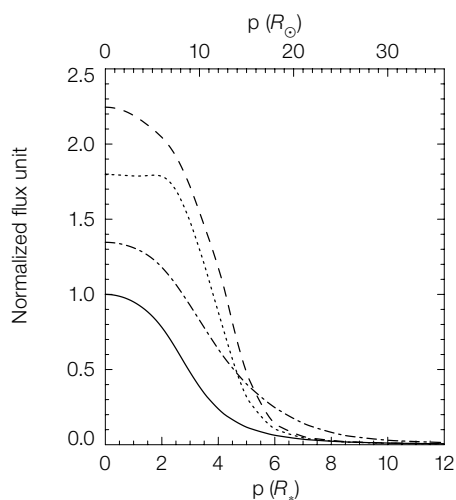
WR stars are characterised by an extra-ordinary hydrogen-deficient spectrum, dominated by broad emission lines of highly ionised elements (such as He II, C IV, N V or O VI). The dense stellar winds completely veil the underlying atmosphere so that an atmospheric analysis can only be done with dynamical, spherically extended model atmospheres, such as those developed by Schmutz et al. (1989), Hillier & Miller (1998), or Gräfener et al. (2002). In the two last decades, significant progress has been achieved in this respect, so that WR stars can be placed on the Hertzsprung-Russell Diagram (HRD) with some confidence (see e.g., Crowther, 2007).

Classification of WR stars is based upon the appearance of optical emission lines of different ions of helium, carbon, nitrogen and oxygen. The nitrogen-rich, or WN-type, is defined by a spectrum in which helium and nitrogen lines (He I–II and N III–V) dominate. In the carbon-rich, or WC-type, helium, carbon, and oxygen lines (C II–IV, He I–II and O III–VI) dominate the emission-line spectrum. Castor, Abbott & Klein (1975) demonstrated that hot-star winds could be explained by considering radiation pressure alone. In this early model, each photon is scattered once at most, and this is sufficient to drive OB-star winds, while more difficulties were encountered for WR stars. Model atmosphere studies have advanced suffi - ciently to enable the determination of stellar temperatures, luminosities, abundances, ionising fluxes and wind proper - ties of WR stars. What remains uncertain are the kinematics of the wind and the wind acceleration law. Furthermore, rotation is very difficult to measure in WR stars, since photospheric features are absent. This parameter is crucial when considering GRBs.

Atmospheric models of WR stars are parameterised by the inner boundary radius R_*, at high Rosseland optical depth (typically above 10), but only the optically thin part of the atmosphere is seen by the observer. Therefore, the

determination of R_* depends on the assumptions made on the velocity law of the wind, considering that typical WN and WC winds have reached a significant fraction of their terminal velocity before they become optically thin in the continuum (especially in the near- and mid-IR). Typical scales for R_* are 3–6 $R_{\odot}$, depending on the spectral sub-type (Crowther, 2007). In the near-IR, the main opacity comes from free–free interactions, and the continuum-forming region is more extended at longer wavelengths, reaching 2–6 R_*. The core radius of WN stars is larger than of WC stars, but the wind of WC stars is denser, and the continuum forms farther away from the core radius. As a consequence, the continuum diameter is about the same, of the order of 10–20 $R_{\odot}$, corresponding to a diameter of about 0.1–0.2 mas for sources at 1 kpc. This implies that the continuum of both WN- and WC-type WR stars remains unresolved for the VLTI in the near-IR, even with the longest (130 m-scale) baselines. Yet, this conclusion does not hold for the line-forming regions (LFR) that can be located at typically 5–50 R_* and that

Figure 1. Left: Simulation of the spatial extent of a WC8 star wind in the continuum at 2.10 μm (solid line) and in three different emission lines (C III 2.11 μm – dash-dotted line; C IV 2.07 μm – dotted line; C IV 2.08 μm – dashed line). The apparent size of the WR star in the emission lines can be as much as twice the continuum size. Right: Simulated images of the same star in the continuum region around 2.10 μm (centre) and in the C IV 2.07 μm line (right). The continuum can be described by a Gaussian intensity distribution, while the superposition of continuum and line flux leads to an intensity distribution that can be described by a limb-darkened disc.

can be resolved by an interferometer, provided that a minimum spectral resolution of 500 is available. Therefore, observing the LFR of WR stars with long-baseline optical interferometry offers the opportunity to probe their winds in the following ways:
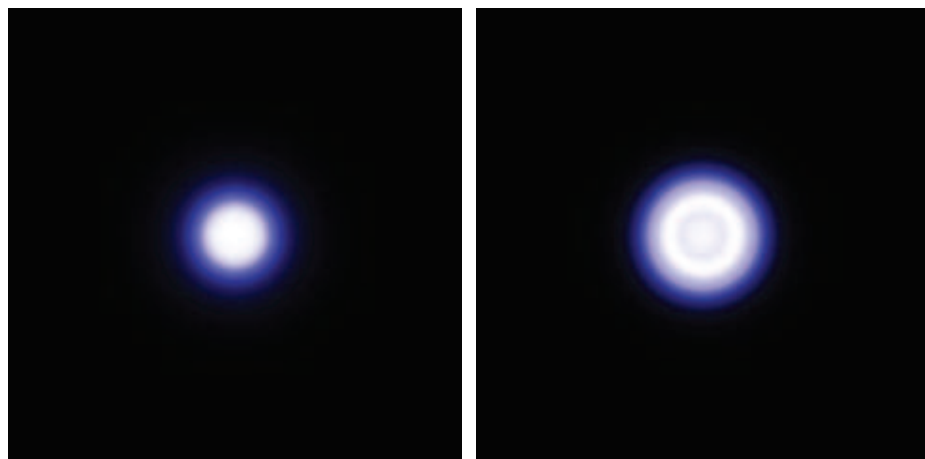
– By measuring the extension of the LFR compared to the continuum. The spatial and kinematical characteristics of the wind can be better inferred and the wind velocity law (especially with access to shorter wavelength data) possibly constrained.

– By examining any deviation from sphericity of these objects. If WR stars were rapid rotators, one would expect strong wavelength-dependent deviations from spherical symmetry, as was detected for the luminous blue variable star η Car with AMBER/VLTI (Weigelt et al., 2007) for example.

– By examining the deviations and perturbations of the WR wind from purely radial motion. Such deviations may originate from dust formation very close to some of these hot stars.

The first, and still most common, method of measuring the angular extent of an astrophysical object with a stellar interferometer is to use an idealised uniform disc to model the stellar photosphere. In reality, WR stars are not "hard-edged" in the continuum, which forms directly in the wind (see Figure 1).

Probing the wind of the closest WR star: γ² Vel

Among all WR stars, γ² Vel is by far the closest, with a well-known distance today of 336 ± 8 pc (North et al., 2007), whilst all others are beyond 1 kpc. Owing to its relative proximity, γ² Vel is relatively bright and has been studied in great detail, mainly using spectroscopy. Through spectroscopic eyes, γ² Vel is shown to be a binary WR + O system (WC8 + O7.5III, P = 78.53 days), thus offering access to the fundamental parameters of the WR star, usually obtained only indirectly through the study of its dense and fast wind. The presence of X-ray emission in the system (Skinner et al., 2001) could be explained by an X-ray-emitting bow-shock between the O-star wind and the WR-star wind (the so-called wind–wind collision zone, [WWCZ]). γ² Vel was observed by the Narrabri intensity interferometer, operating at around 0.45 μm, as early as 1968 (Hanbury Brown et al., 1970), but since the observations lacked spectral resolution, they could not resolve the WWCZ.

Our team observed γ² Vel in December 2004 using the AMBER/VLTI instrument with the aim of constraining various parameters of the system, such as the brightness ratio of the two components, the spectral and spatial extent of the WWCZ, and the angular size associated with both the continuum and the lines emitted by the WR star. AMBER delivered spectrally dispersed visibilities as well as differential and closure phases and, of
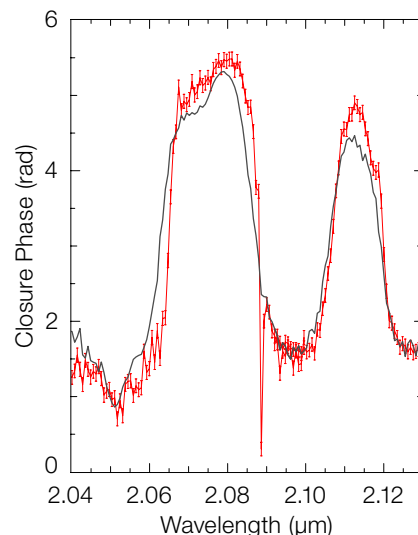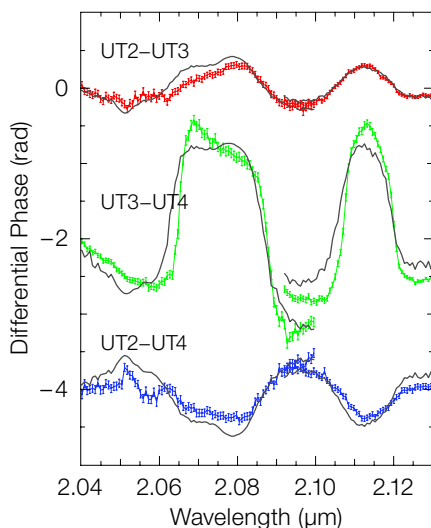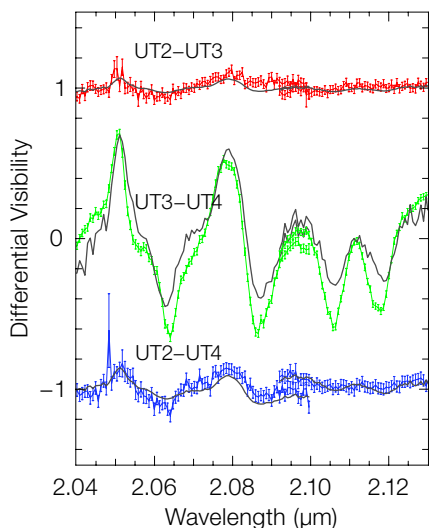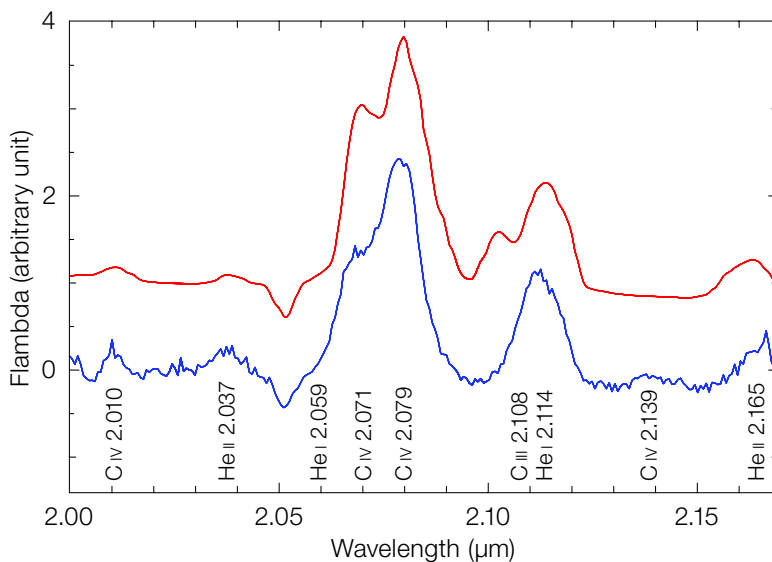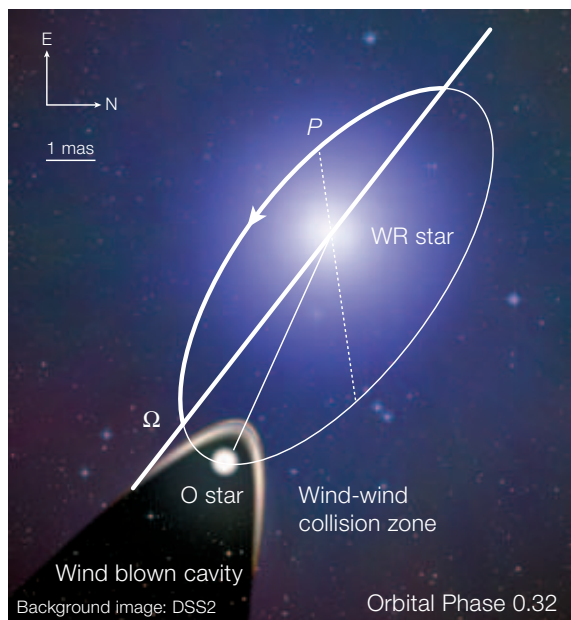
course, also a spectrum of the object. During these observations, AMBER worked with a resolution of R = 1500 in the spectral band 1.95–2.17 μm. We inter-preted the AMBER data in the context of a binary system with unresolved components, neglecting, to a first approxi-mation, the wind–wind collision zone flux contribution and the extension of the WR wind (Millour et al., 2007). Based on the accurate spectroscopic orbit and the Hipparcos distance (258 $^{+41}_{-31}$ pc), the expected separation at the time of the observations was 5.1 ± 0.9 mas. How-ever, our observations showed that the Hipparcos distance was incorrect

since we observed a separation of 3.62 $^{+0.11}_{-0.30}$ mas, implying a distance of 368 $^{+38}_{-13}$ pc, which is in agreement with recent spectrophotometric estimates. An independent observation by the Sydney University Stellar Interferometer (SUSI) confirmed and refined the distance estimate of γ^2 Vel at 336 $^{+8}_{-7}$ pc (North et al., 2007).

In contrast to SUSI, which uses broad-band filters, AMBER allowed us to dis-perse the K-band light with a resolution of 1500. Therefore, we were able to sepa-rate the spectra of the two components; i.e., we obtained, for the first time, an

independent spectrum of the WR com-ponent of γ^2 Vel in the K-band. This allowed us to compare the WR spectrum with line-blanketed radiative transfer models of WR stars (Dessart et al., 2000). The match between the inferred WR spectrum and the modelled spectrum is

Figure 2. γ^2 Vel as seen by AMBER in 2004 (Millour et al., 2007): the observations (lower plots) are fitted successfully by a model involving a WR star and an O star (grey lines). One can extract the spectrum of the Wolf-Rayet star alone from this model-fitting (top-right panel, blue curve) and compare it with a radiatively-driven WR wind model spectrum (red curve). The general view of the system (top-left) also involves a wind–wind collision zone.

relatively good, except for some regions where the match is worse (especially in a few emission lines and in some parts of the continuum, see Figure 2). This suggests that as a second order perturbation, an additional light source in the system may affect our fit. We checked that this marginal mismatch cannot come from a flat continuum emission, and therefore, we favoured the presence of an additional compact light source in the system.

After that first study, we carried out follow-up observations of γ^2 Vel in 2006 and 2007. In addition to a refinement of the orbital solution of North et al., (2007), Millour et al. (2008) were able to locate

this additional light source in the system between the two main stars. If this source is confirmed, it would be located closer to the O star than to the WR star and would contribute approximately 5% of the total flux of the system (i.e., additional free–free emission). This is in agreement with the expectations from Millour et al. (2007) and, possibly, we have detected the wind–wind collision zone (WWCZ) between the two stars.

However, other effects, such as the LFR extent, can also affect our interferometric signal. Indeed, in the past, different velocity laws were used for models of γ^2 Vel, e.g., a steep velocity law or a combined

law with a steep inner region and a flat outer region. Leaving aside the technical details, this basically implies that different velocity laws predict a different extent of the LFR. Therefore, we are currently continuing our investigations on γ^2 Vel with the VLTI to disentangle better the different light contributions in this fascinating system.

The dust formation puzzle

One challenging problem related to WR stars is understanding how dust can form in the hostile environment of these hot stars. It turns out that several of the dusty WR stars harbour a so-called pinwheel nebula, as shown recently by the observations of Tuthill et al. (see, for example, their article in 2008). From an interferometric point of view, pinwheel nebulae appear in the visibilities as typical whirlpool modulations that can be detected with the current performance of the VLTI (see Figure 3). When the number of datasets is very limited, clues to the presence of a pinwheel can also come from a plateau-like shape in the visibilities towards longer baselines. Of course the detection of new pinwheel nebulae would provide a more direct evidence of the binarity of the observed stars, but a clear detection of the underlying binary in known pinwheels is also one of the goals of studying these dusty WR stars. Up to now, we have successfully observed a few dusty
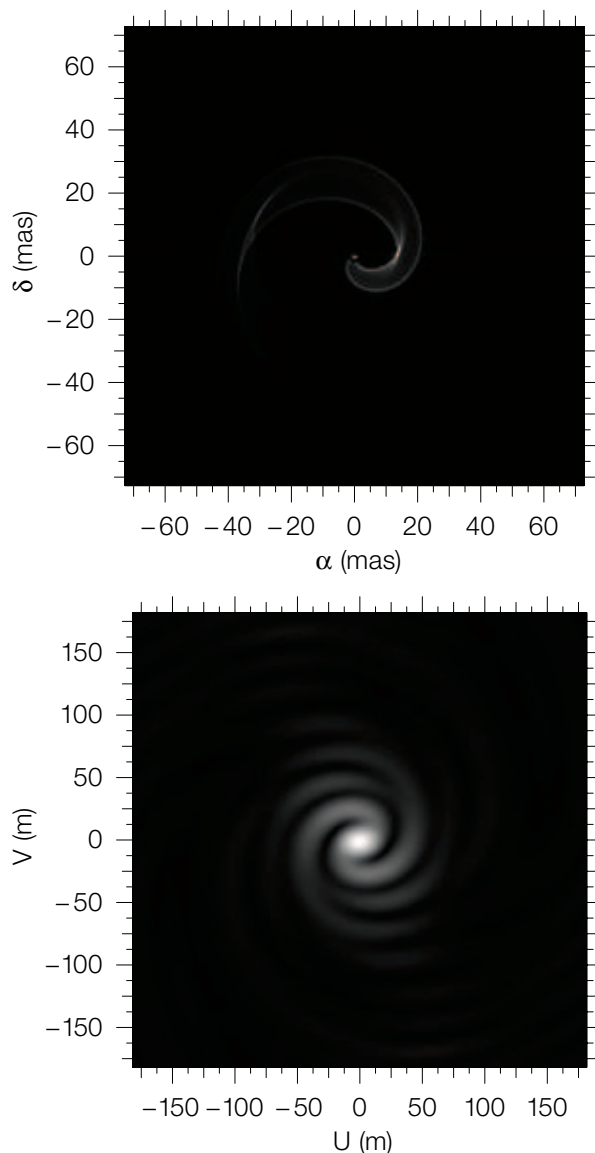

Figure 3. What kind of visibility signature can we expect from a pinwheel nebula? This example using a pinwheel "toy model" (top-left) illustrates the whirlpool shape of the 2D visibility map (bottom-left) as well as the plateau-like shape of the visibilities towards longer baselines, as seen from the radial cuts in the bottom-right panel. A two-component Gaussian is also shown for comparison. These two characteristic visibility signatures provide clues to the presence of a pinwheel around a dusty WR star.
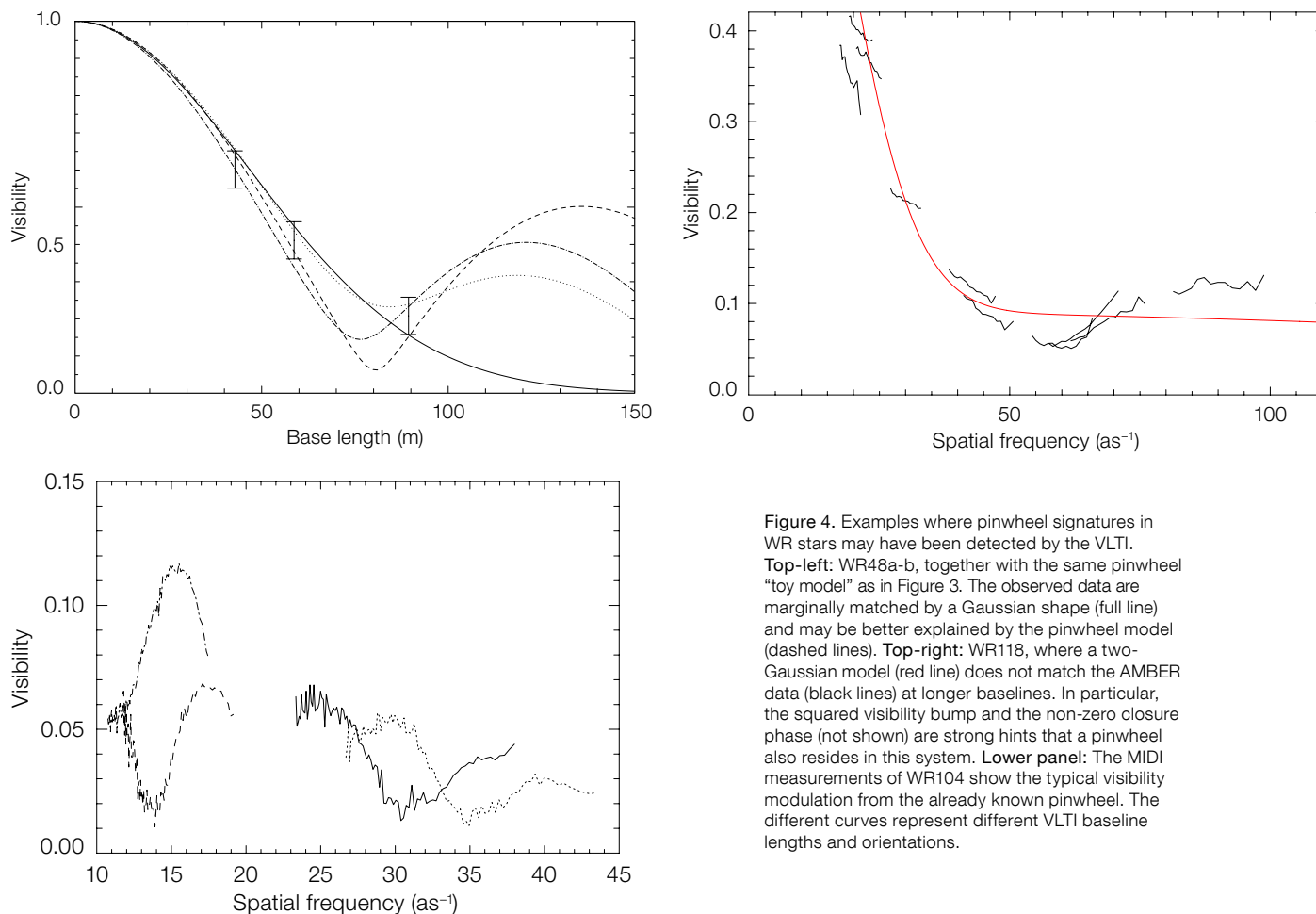
Figure 4. Examples where pinwheel signatures in WR stars may have been detected by the VLTI. **Top-left:** WR48a-b, together with the same pinwheel "toy model" as in Figure 3. The observed data are marginally matched by a Gaussian shape (full line) and may be better explained by the pinwheel model (dashed lines). **Top-right:** WR118, where a two-Gaussian model (red line) does not match the AMBER data (black lines) at longer baselines. In particular, the squared visibility bump and the non-zero closure phase (not shown) are strong hints that a pinwheel also resides in this system. **Lower panel:** The MIDI measurements of WR104 show the typical visibility modulation from the already known pinwheel. The different curves represent different VLTI baseline lengths and orientations.

Wolf-Rayet stars with the VLTI, which illustrates the potential of optical/IR interferometry to contribute to the fascinating question of the binarity of these stars.

WR 48a is a WC star producing dust in the form of eruptions, which suggests the presence of a companion. It is found to be within 1 arcsecond of the two heavily reddened, optically visible clusters Danks 1 and 2, which are themselves separated by only 2 arcseconds. Another object that also seems to be a dusty WR star (MSX6C G305.4013 + 00.0170) was found close to WR48a, which we hereafter denote as WR48a-b. No optical counterpart is reported in the literature and the JHK photometry for this source from the Two Micron All Sky Survey (2MASS) shows a spectral shape indicative of an object with high extinction (A_V ~ 10 mag). WR48a and WR 48a-b were successfully observed with the

AMBER/VLTI instrument. Both objects have angular diameters of about 4–6 mas in the K-band and mid-IR sizes of the order of 10–15 mas. The sizes measured are quite large, compared to the expected size of single WR stars (0.1–0.5 mas), and these two objects are probably two good candidates to harbour pinwheel nebulae, even though no clear signature has been formally detected yet (Figure 4). These two targets are definitely inter - esting because they produce dust and, hence, are likely binary candidates, belonging to a young star-forming region whose distance is more accurately known than is usual for WR distances.

WR 118 is a highly evolved, carbon-rich Wolf-Rayet star of spectral type WC10. It is the third brightest Wolf-Rayet star in the K-band (K = 3.65), and its large IR-excess is attributed to an envelope com-posed of carbonaceous dust. Since no

remarkable changes in the dust emission have been observed in the past two dec-ades, WR 118 is classified as a permanent dust producer. The extended dust enve-lope of WR 118 was successfully resolved for the first time by Yudin et al. (2001) using bispectrum speckle interferometry with the 6-metre BTA (Large Altazimuth Telescope). Yudin et al. concluded that the apparent diameter of WR 118's inner dust shell boundary is 17 ± 1 mas. We recently measured WR 118 with AMBER in low-spectral resolution mode (see Figure 4). At first glance, the AMBER visibilities sug - gest that there is an unresolved compo-nent contributing approximately 15% to the total K-band flux. In addition, one can see that the K-band visibility is not spheri-cally symmetric, and we detected non-zero closure phases. These clues illustrate that the overall shape of the measured visibility of WR 118 is in qualitative agree-ment with the visibility signature expected

from a spiral-like dust distribution. Currently, the interpretation of the recently obtained AMBER data is being subjected to a more detailed analysis.

The most recent dusty WR star observed with the VLTI so far was WR 104 with the MIDI instrument. WR 104 is the archetype of the colliding-wind binary creating a beautiful pinwheel system, which was first detected by the technique of aperture masking with the Keck telescope (Tuthill et al., 2008). We observed it with MIDI using two of the auxiliary telescopes. The visibilities show the signature of two flux distributions on the source: a Gaussian-shaped dusty envelope surrounding the binary system and producing 80–90% of the flux in the mid-infrared, and the dust pinwheel. The characteristic pinwheel signal is seen by MIDI as a cosine modulation, evolving with time as the pinwheel rotates and the interferometer baseline length and orientation change (see Figure 4). Such a limited amount of data would be extremely difficult to interpret if the global geometry and the ephemeris of this source were not accurately known. These observations promise to evaluate precisely the size of the dust-forming region and the dust production of the system, as viewed at high spatial resolution.

Prospects

The studies described correspond to work in progress with the VLTI for observing WR stars. No imaging of these sources has been done up to now, but the AMBER instrument, with three telescopes combined, has some imaging capabilities. A first image of a pinwheel, with resolutions much higher than single pupil telescopes, would be a milestone in IR long-baseline interferometric research on dusty WR stars and would probably trigger more VLTI observing programmes in this field. On the other hand, reaching sufficient dynamic range with AMBER/VLTI in medium spectral resolution mode, would allow one to directly constrain the WR wind velocity field in the emission lines. Observing with shorter wavelengths (H or J bands, or even visible), would boost this research field, as both the interferometer resolution and the LFR extent increase towards shorter wavelengths. This would open the possibility to directly validate the competing models for WR winds or, maybe, could even lead to new and unexpected results.

References

Crowther, P. A. 2007, ARA&A, 45, 177
Castor, J. I. et al. 1975, ApJ, 195, 157
Dessart, L. et al. 2000, MNRAS, 315, 407
Gräfener, G. et al. 2002, A&A, 2002, 387, 244
Hanbury Brown, R. et al. 1970, MNRAS, 148, 103
Hillier, D. J. & Miller, D. L. 1998, ApJ, 496, 407
Millour, F. et al. 2007, A&A, 464, 107
Millour, F. et al. 2008, SPIE, 7013
North, J. R. et al. 2007, MNRAS, 377, 415
Schmutz, W. et al. 1989, A&A, 210, 236
Skinner S.L. et al. 2001, ApJL, 558, 113
Tuthill, P. G. et al. 2008, ApJ, 675, 698
van der Hucht, K. A. 2001, New Astronomy Review, 45, 135
Weigelt, G. et al. 2007, A&A, 464, 87
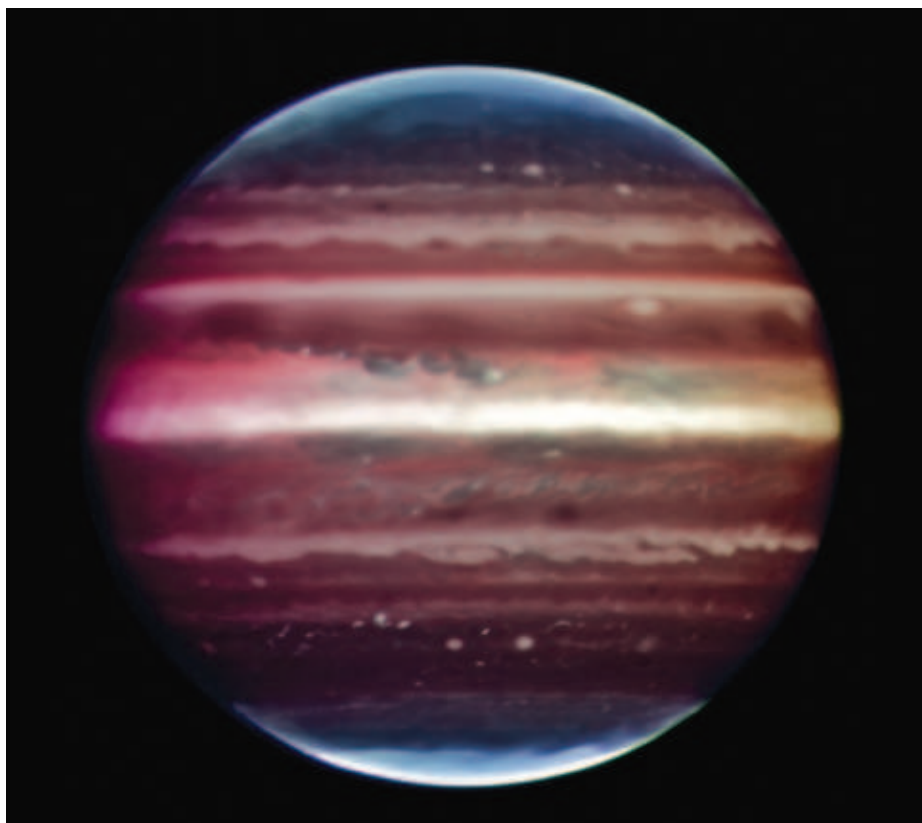Yudin, B. et al. 2001, A&A, 379, 229

Image of Jupiter taken in near-infrared light with the VLT Multi-conjugate Adaptive optics Demonstrator (MAD) prototype instrument on 17 August 2008. This colour composite is formed from a series of images taken over a time span of about 20 minutes, through three filters at 2.2 μm (Ks-band), 2.14 μm (Brackett-γ continuum) and 2.17 μm (Brackett-γ). The filters select hydrogen and methane absorption bands. The spatial resolution is about 90 milliarcseconds across the whole disc, corresponding to 300 km on the planet surface. See ESO PR 33/08 for more details